Article

Current Biology

Reciprocal Fitness Feedbacks Promote the Evolution of Mutualistic Cooperation

Graphical Abstract

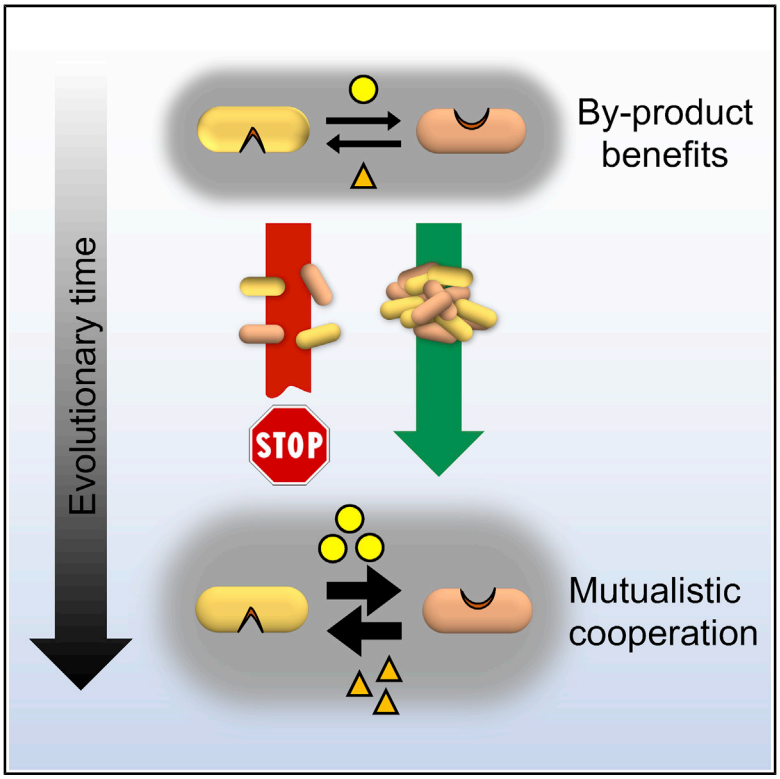

Authors

Daniel Preussger, Samir Giri, Linéa K. Muhsal, Leonardo Oña, Christian Kost

Correspondence

christiankost@gmail.com

In Brief

Preussger et al. experimentally evolve a costly mutualistic cooperation in a spatially unstructured environment. They identify positive fitness feedbacks within aggregated groups as the causal mechanism driving the evolution of cooperation. These results suggest the evolution of mutualistic cooperation is less challenging than previously thought.

Highlights

- Mutualistic cooperation can evolve in a spatially unstructured environment
- Spatial clustering and reciprocal fitness feedback drive the evolution of cooperation
- Non-cooperators are less fit than cooperative individuals

Preussger et al., 2020, Current Biology *30*, 3580–3590
September 21, 2020
https://doi.org/10.1016/j.cub.2020.06.100

CellPress

CellPress

Current Biology

Article

Reciprocal Fitness Feedbacks Promote the Evolution of Mutualistic Cooperation

Daniel Preussger,[1,2,3] Samir Giri,[1,2,3] Linéa K. Muhsal,[2,3] Leonardo Oña,[2] and Christian Kost[1,2,4,*]

[1]Experimental Ecology and Evolution Research Group, Department of Bioorganic Chemistry, Max Planck Institute for Chemical Ecology, Beutenberg Campus, Hans-Knöll Str. 8, Jena 07745, Germany

[2]Department of Ecology, School of Biology/Chemistry, University of Osnabrück, Osnabrück 49076, Germany

[3]These authors contributed equally

[4]Lead Contact

*Correspondence: christiankost@gmail.com

https://doi.org/10.1016/j.cub.2020.06.100

SUMMARY

Mutually beneficial interactions are ubiquitous in nature and have played a pivotal role for the evolution of life on earth. However, the factors facilitating their emergence remain poorly understood. Here, we address this issue both experimentally and by mathematical modeling using cocultures of auxotrophic strains of *Escherichia coli*, whose growth depends on a reciprocal exchange of amino acids. Coevolving auxotrophic pairs in a spatially heterogeneous environment for less than 150 generations transformed the initial interaction that was merely based on an exchange of metabolic byproducts into a costly metabolic cooperation, in which both partners increased the amounts of metabolites they produced to benefit their corresponding partner. The observed changes were afforded by the formation of multicellular clusters, within which increased cooperative investments were favored by positive fitness feedbacks among interacting genotypes. Under these conditions, non-cooperative individuals were less fit than cooperative mutants. Together, our results highlight the ease with which mutualistic cooperation can evolve, suggesting similar mechanisms likely operate in natural communities.

INTRODUCTION

Mutually beneficial interactions are ubiquitous in nature and highly diverse in form and function [1, 2]. By providing organisms with new phenotypic traits, mutualistic interactions represent an important source of evolutionary innovation that has been key to the diversification of life on earth [3–6]. Because of their ability to produce a broad range of different metabolites, bacteria are frequently involved in mutualistic interactions with both other bacteria and eukaryotic hosts [7–9].

The evolution and maintenance of cooperative metabolic interactions, however, pose a fundamental problem [10–12]: why should one organism invest costly resources to benefit another individual and not use them to enhance its own fitness? Evolutionary theory predicts non-cooperating individuals that reap benefits without reciprocating gain a significant fitness advantage over types carrying the burden of an increased cooperative investment [13]. This asymmetry represents not only a major hurdle for the *de novo* evolution of mutualistic cooperation but also a constant threat for its persistence in the long run [14, 15].

One possible solution that could explain the evolution of cooperative metabolic mutualisms are localized interactions in spatially structured environments [16–18]. This hypothesis is based on the idea that because of limited dispersal, two individuals colocalize in close spatial proximity. If both parties reciprocally exchange synergistic benefits, any emerging mutant that increases its investment into the traded commodity will immediately gain an advantage: facilitating the growth of its partner should also increase the benefits it receives in return. As a consequence of the resulting fitness feedbacks, selection should favor cooperation and thus intensify the interaction on both sides [19]. The simplicity of this idea that does not assume any prior adaptations, combined with the fact that the vast majority of bacterial life exists in spatially structured communities [20, 21], make this hypothesis particularly appealing.

Despite the plausibility of the above scenario, several factors might also oppose an intensification of the ancestral synergistic interaction. First, spatial structure can enhance competition for nutrients [22–26] or compound detrimental effects resulting from the secretion of toxic waste products [27], thus hindering cooperation [28, 29]. Second, insulation effects within densely packed cell groups can prevent metabolic exchange among synergistic partners [30, 31]. Third, spatial structures formed by microbial communities are likely transient, yet undergo intermittent phases of dissolution and restructuring. The ensuing mixing of cells can constrain repeated encounters of complementary types in subsequent rounds of interaction [32].

Here, we use an experimental evolution approach to test whether cooperation evolves between two synergistic bacterial genotypes and if so, which evolutionary mechanism can explain its emergence. To this end, we cocultured pairs of auxotrophic genotypes of the bacterium *Escherichia coli* that could only grow when they reciprocally exchanged essential amino acids. Thus, the interaction was initially based on a trading of byproducts that were not produced to benefit the corresponding partner. Given that nutrient-starved bacterial genotypes frequently

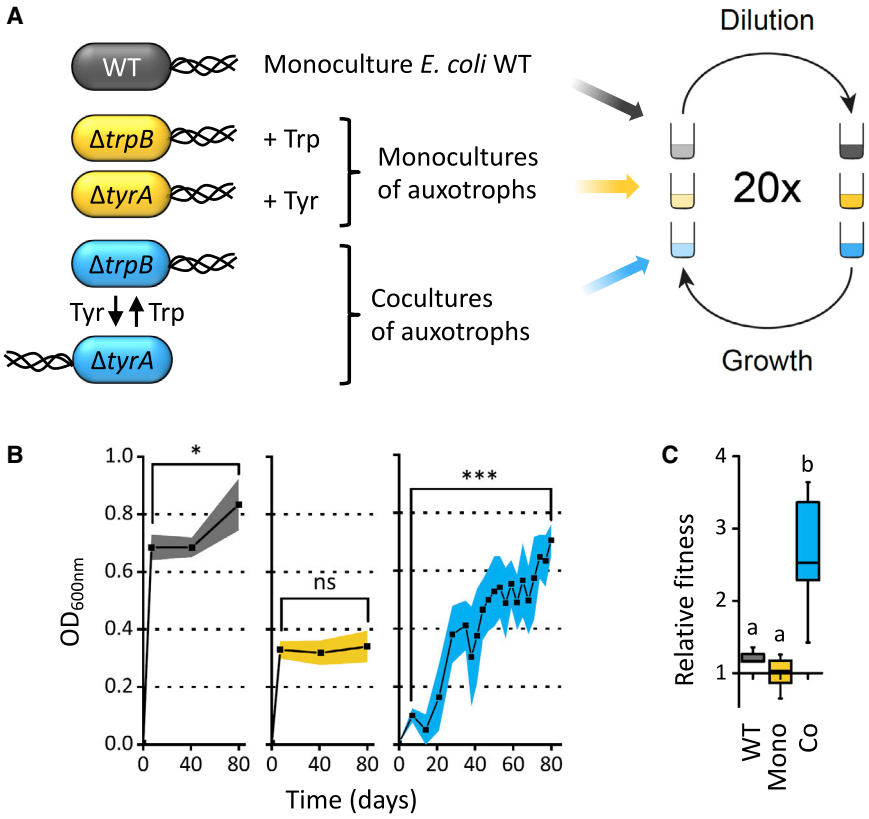

Figure 1. Productivity and Fitness Significantly Improved in Cocultures of Auxotrophs

(A) Design of the evolution experiment. Three experimental groups (i.e., monocultures of prototrophic wild type (WT), monocultures of auxotrophic genotypes (Mono) supplemented with the two amino acids tyrosine (+Tyr) and tryptophan (+Trp), and cocultures of auxotrophic genotypes of *Escherichia coli* (Co) were serially propagated for 80 days in shaken liquid medium.

(B) Mean population density (±95% confidence intervals) quantified as optical density (OD_{600nm}) over the course of the evolution experiment. WT monocultures and auxotrophic cocultures significantly increased in optical densities, whereas the growth level of monocultures of auxotrophs remained unchanged (paired sample t test comparing optical densities after 7 days and 80 days of incubation, WT: *$p < 0.05$, $t = -2.805$, $n = 12$; Mono: ns $p = 0.69$, $t = -0.397$, $n = 19$; Co: **$p < 0.001$, $t = -17.365$, $n = 10$).

(C) Change in Darwinian fitness of derived populations relative to their evolutionary ancestors. Relative fitness is the net growth of derived consortia divided by the growth achieved by the corresponding ancestors during a 72-h period. Ancestral and derived populations were cultivated separated from each other. Different letters indicate significant differences (ANOVA followed by a least significant difference (LSD) post hoc test: $p < 0.001$, $F = 35.033$, $df = 34$ (WT: $n = 6$, Mono: $n = 19$, Co: $n = 10$)). Relative fitness of WT and Co is significantly different to 1 (one-sample t test, WT: $p < 0.05$, $t = 23.75$, $df = 5$, Co: $p < 0.001$, $t = 10.25$, $df = 9$), whereas the one of Mono is not (one-sample t test, Mono: $p > 0.05$, $t = 0.56$, $df = 18$). See also Figures S1 and S2.

aggregate to enhance metabolic exchange [33–39], we hypothesized that the resulting spatial structures should also facilitate the evolution of metabolic cooperation. For this, genotypes should start to actively increase the amount of amino acid they produce to benefit their corresponding partner. Moreover, this increased investment should be costly to the producing cell yet beneficial in the context of the interaction. As a control, we used monocultures of auxotrophs that were supplemented with the required amino acid as well as populations of the metabolically autonomous wild type (WT; i.e., prototroph). All of these cultures were serially propagated in a rapidly shaken liquid environment to facilitate mixing among genotypes.

Our results show that a costly cooperative exchange of amino acids rapidly evolved in serially propagated cocultures of auxotrophic genotypes but not in monoculture controls. The evolution of cooperative cross-feeding was due to the formation of multicellular clusters that were essential for an efficient transfer of amino acids among cells. Finally, we demonstrate that despite significant fitness costs, cooperation was strongly favored when cells were part of a collective but not when they were experimentally excluded from multicellular clusters. Taken together, our data show that reciprocal fitness feedbacks within dynamic and self-organized multicellular clusters drive the evolution of metabolic cooperation within auxotrophic bacterial communities.

RESULTS

Design of the Evolution Experiment

To determine whether a cooperative metabolic interaction can evolve from an interaction that initially depends on a reciprocal exchange of byproducts, an evolution experiment was conducted using three different treatment groups (Figure 1A). First, prototrophic WT cells of *Escherichia coli* were serially propagated in minimal medium. Second, two auxotrophic genotypes of *E. coli* (i.e., Δ*tyrA* and Δ*trpB*) that each lacked the ability to autonomously produce one amino acid (i.e., tyrosine [Tyr] or tryptophan [Trp]) were cultivated in monoculture in a minimal medium that contained the amino acid each strain required for growth in non-saturating concentrations (i.e., 50 μM, Mono). Third, the two auxotrophic genotypes were cocultured in a minimal medium without amino acid supplementation (Co). Under these conditions, the two auxotrophic mutants showed marginal growth (Figures 1B and S1), which was likely due to a reciprocal exchange of essential amino acids. This experimental design aimed at testing whether serial propagation of cocultured auxotrophs favored the evolution of metabolic cooperation, while this should not be the case in monocultures of auxotrophic and prototrophic WT cells. Twelve replicate populations of each experimental group were serially propagated for a total of 20 cycles of growth and subsequent dilution into fresh minimal medium

(Figure 1A). Populations were initially transferred every 7 days. However, because cocultures of auxotrophs rapidly increased in growth, the transfer interval of all three treatment groups was reduced to 3 days after the fifth cycle.

Cocultures of Auxotrophs Rapidly Improved in Fitness

Following the evolution experiment, we first tested whether auxotrophic genotypes had reverted to a prototrophic phenotype [40]. Plating all derived populations on amino acid-deficient agar plates revealed that in 10 populations of cocultured auxotrophs, both cell types were present and still auxotrophic at the end of the evolution experiment. However, two populations completely consisted of reverted phenotypes that had re-evolved the ability for prototrophic growth. This observation indicates that these populations have found an alternative solution to overcome the growth limitation imposed by the metabolic auxotrophy. However, in the context of the current study, these replicates as well as their cognate controls (i.e., auxotrophic monocultures) were excluded from further analysis.

To determine whether or not the growth of the three different treatment groups increased over the course of the evolution experiment, the optical density they reached after a growth cycle was quantified at different time points. Comparing the growth each of the three groups reached at the beginning, with the one they achieved at the end of the experiment, revealed a marginal but significant increase in the case of WT populations (1.2-fold; Figure 1B), whereas the growth of auxotrophic control populations remained unchanged (1.04-fold; Figure 1B). In contrast, cocultures of auxotrophs showed a much stronger increase in growth (7-fold; Figure 1B) and finally reached levels that were statistically indistinguishable from those of the ancestral WT populations (independent sample t test: $p = 0.6$, $t = -0.531$, $n \geq 10$).

A similar pattern emerged when the net improvement in growth (i.e., a measure of fitness) was directly compared between derived cultures and their evolutionary ancestors: both WT and cocultures of auxotrophs significantly increased in fitness (one-sample t test WT: $p < 0.05$, $t = 23.751$, $n = 6$; CO: $p < 0.001$, $t = 10.247$, $n = 10$), whereas the fitness of monocultures of auxotrophs remained unchanged (one-sample t test Mono: $p = 0.582$, $t = 0.560$, $n = 19$; Figure 1C). Strikingly, the fitness increase of cocultures (2.5-fold) was significantly higher than the ones of the prototrophic WT (1.2-fold, independent sample t test: $p = 0.005$, $t = -3.281$, $n \geq 6$). Together, these results indicate that the synergistic coevolution experienced by auxotrophic types in coculture enhanced their rate of adaptation relative to the two control groups that were capable of independent growth.

Coevolved Auxotrophs Diversified Morphologically

Plating ancestral and derived populations on indicator agar plates, which were used to distinguish individual genotypes, revealed noticeable changes in the colony morphologies (Figure S2): in 8 out of 10 cocultures of derived auxotrophs (i.e., 80%), at least one of the two partners contained mutants that showed a colony morphology, which clearly differed from the one of its evolutionary ancestor in terms of colony size and color. In contrast, only 3 out of 19 auxotrophic monocultures analyzed (i.e., 16%) contained novel morphotypes, whereas none of the derived WT populations (i.e., 0%) showed an apparent change in their colony morphology. Thus, the probability of phenotypic diversification was significantly increased in derived cocultures (chi-square test: $p = 0.04$, $\chi^2 = 4.23$, $df = 1$), whereas it could not be distinguished from chance in the two control groups (Mono: chi-square test: $p = 0.28$, $\chi^2 = 1.15$, $df = 1$). To consider this variation in subsequent experiments, four representatives of each identified morphotype were isolated.

The Fitness Increase of Cocultured Auxotrophs Was Due to the Evolved Overproduction of Exchanged Amino Acids

The strongly enhanced growth observed in derived cocultures suggested both parties have increased the amount of amino acids they produced to support the growth of their corresponding partner. Two different mechanisms are known of how bacteria can transfer amino acids between cells [41]: first, via diffusion through the extracellular environment or second, using contact-dependent structures to derive cytoplasmic metabolites from other bacterial cells (e.g., nanotubes) [34, 42]. Thus, to quantify the total amount of amino acids that is being transferred between cells via both diffusion and contact-dependent mechanisms, derived clones as well as their corresponding evolutionary ancestors of all three treatment groups were individually cultivated in a medium that contained the amino acid they essentially required for growth. At the same time, a second genotype of *E. coli*, which was auxotrophic for the focal amino acid (i.e., Tyr or Trp), was co-inoculated into the same cultures. Here, the auxotrophic recipients served as an amino acid biosensor, whose growth correlates with the amount of the focal amino acid, produced by the donor strain [43].

Comparing amino acid production rates of derived clones relative to the levels of their evolutionary ancestors in this way revealed a significantly increased production of Tyr and Trp in coevolved auxotrophs (Mann-Whitney U test: $p = 0.002$, $Z = -3.171$, evolved auxotrophs: $n = 420$, ancestral auxotrophs: $n = 60$; Figure 2A). In contrast, auxotrophic monocultures showed the opposite trend of producing significantly less amino acids than their evolutionary ancestors (Mann-Whitney U test: $p < 0.001$, $Z = -3.541$, evolved auxotrophs: $n = 264$, ancestral auxotrophs: $n = 57$), whereas in the prototrophic WT, these measures remained unchanged for both Trp (Mann-Whitney U-test: $p = 0.220$, $Z = -1.228$, $n = 72$) and Tyr (Mann-Whitney-U-test: $p = 0.112$, $Z = -1.588$, $n = 72$; Figure 2A). Additionally, comparing absolute biosensor-to-donor ratios confirmed these differences and clearly showed that coevolved auxotrophs produced significantly more amino acids than derived control groups (ANOVA followed by a Dunnett's T3 post hoc test: $p < 0.01$, $F = 5.286$, $df = 335$ for recipient Δ*tyrA* and $p < 0.001$, $F = 29.244$, $df = 335$ for recipient Δ*trpB*; Figure S3A).

Finally, correlating the amount of amino acids coevolved auxotrophs produced with the fitness the corresponding consortia achieved over the course of the evolution experiment revealed a strong and significant positive relationship between both measures (Spearman rank correlation: $p < 0.01$, $rho = 0.404$, $n = 60$; Figure 2B). This observation clearly shows that the fitness increase observed in populations of cocultured auxotrophs (Figures 1B and 1C) was driven by enhanced production levels of the amino acids that were exchanged among interacting strains.

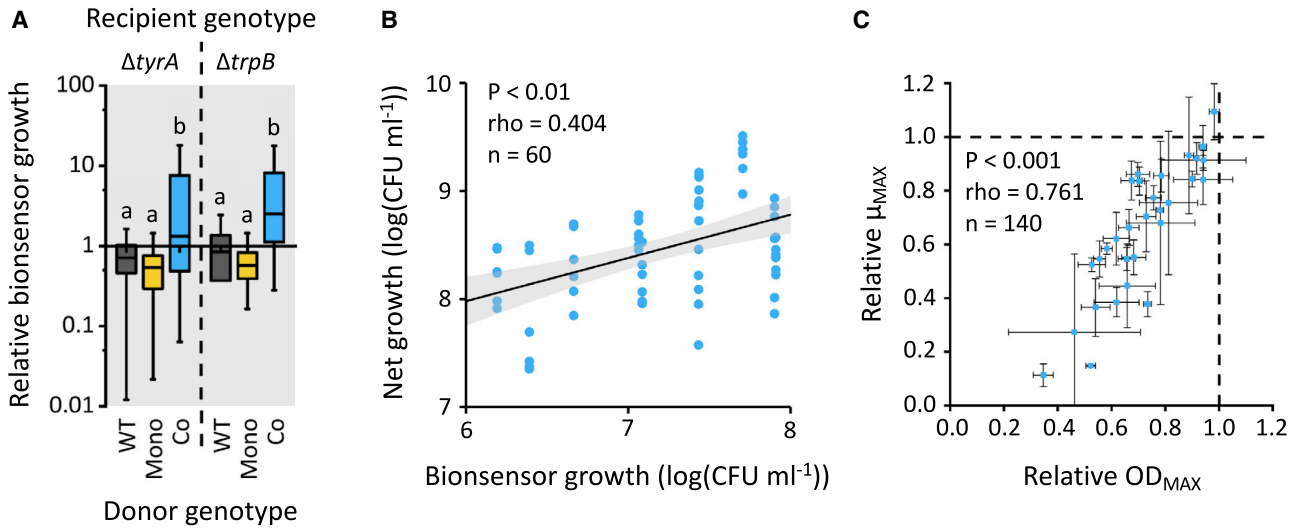

Figure 2. Cocultured Auxotrophs Evolved a Costly Overproduction of the Exchanged Amino Acids

(A) Coevolved auxotrophs, but not isolates of monoculture controls, produce increased amounts of the exchanged amino acid. Shown is the ability of derived strains to support the growth of a cocultured auxotroph (Δ*tyrA*: auxotrophic for tyrosine, Δ*trpB*: auxotrophic for tryptophan) relative to the corresponding evolutionary ancestor. Growth of the auxotrophic biosensor, which mirrors the amount of amino acid that is produced by the focal donor, was normalized for the growth of the cocultured donor genotypes. Different isolated morphotypes of evolved populations (n_{WT} = 12, n_{Mono} = 88, n_{Co} = 140) and ancestors (n_{WT} = 12, n_{Mono} = 19, n_{Co} = 20) were used. The whole experiment was replicated three times. Different letters indicate significant differences between groups (ANOVA followed by a Dunnett's T3 post hoc test: Δ*tyrA*: $p < 0.01$, $F = 5.471$, $df = 419$; Δ*trpB*: $p < 0.001$, $F = 51.235$, $df = 335$).

(B) Net growth of consortia of coevolved auxotrophs is positively correlated with the amount of amino acids their constituents produce. Consortia growth was determined during a 3-day period, and amino acid production was quantified as in (A). A linear regression was fitted to the data (black line; grey area: ±95% confidence interval). The result of a Spearman rank correlation is shown.

(C) Coevolved auxotrophs pay a cost of adaptation. Growth of 30 coevolved auxotrophs and their corresponding ancestors was determined in amino acid-supplemented minimal medium. The maximum optical density (OD_{MAX}) and maximum growth rate (μ_{MAX}) achieved is displayed as mean (±95% confidence intervals) ratios of evolved isolates relative to their evolutionary ancestor (n = 4). Dashed lines indicate ancestral levels. A significant Spearman rank correlation between μ_{MAX} and OD_{MAX} points toward a true fitness cost.

See also Figures S3 and S4.

Together, these results show that auxotrophic genotypes, which evolved in coculture, started to produce increased amounts of amino acids—most likely to support the growth of their respective partner. The fact that this was not observed in the two control groups suggests the obligate metabolic interaction was driving this pattern.

Adaptation to Coevolved Partner Is Costly

Given that the coevolved auxotrophic genotypes significantly increased their amino acid production levels, we hypothesized that this elevated energetic investment into the corresponding interaction partners should incur fitness costs to the overproducing cells. To test this, the growth performance of isolates derived from auxotrophic cocultures was compared to the one of their corresponding ancestor using minimal medium, to which the required amino acid has been supplemented in sufficient amounts (i.e., 150 μM for both Tyr and Trp). Strikingly, despite supplementation with high concentrations of amino acids, the growth performance of virtually all derived auxotrophs was consistently below the level of the ancestral auxotrophs (Figure 2C). The only exception to this was one isolate whose maximum growth rate improved in the course of the evolution experiment by around 10% (Figure 2C). This result implies that adaptation to the coevolved partner, which included an increased production of the exchanged amino acid (Figure 2A), incurred a significant fitness cost to coevolved auxotrophs. The fact that both the maximum growth rate and the maximum optical density reached were positively correlated with each other (Spearman rank correlation: $p < 0.001$, rho = 0.761, n = 140) points toward a true fitness cost and rules out the possibility of a rate-yield trade-off. Moreover, the tremendous degree of variation that was observed among isolates (Figure 2C) suggests the different morphotypes likely pursued divergent evolutionary trajectories to evolve mutualistic cooperation. Finally, determining the statistical relationship between the degree of amino acid overproduction (Figure 2A) and the cost of adaptation (Figure 2C) revealed a strongly negative association for both the maximum growth rate (Spearman rank correlation: $p < 0.01$, rho = −0.248, n = 140; Figure S3B) and the maximum optical density achieved (Spearman rank correlation: $p < 0.001$, rho = −0.234, n = 140; Figure S3C). This result suggests that the drastic differences in the quantified cost of adaptation among isolated genotypes can—at least partly—be attributed to the cost of amino acid overproduction.

Cocultures of Auxotrophs Predominantly Interact within Multicellular Clusters

One possible mechanism to account for the observed evolution of a mutualistic cooperation is that cells have formed multicellular aggregates [33–39]. These spatial structures would not

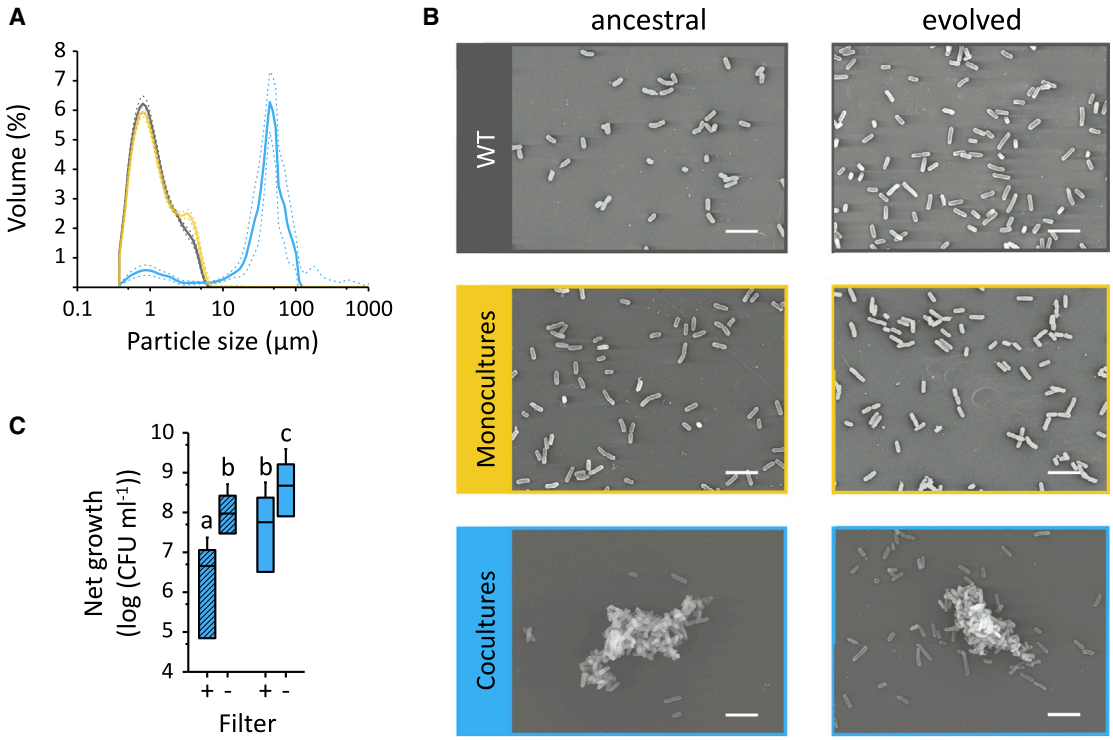

Figure 3. Cocultured Auxotrophs Form Multicellular Clusters

(A and B) Multicellular clusters form in coevolved auxotrophs but not the two control groups. (A) Cumulative size distribution in volume percent of derived populations of WT (gray line, n = 12), monoculture of auxotrophs (yellow, n = 24), and cocultures of auxotrophs (blue, n = 30) during the exponential growth phase as determined by laser diffraction spectroscopy. Each measurement has been replicated three times. Lines are medians and dotted lines represent 95% confidence intervals. Particles with a size >10 μm were considered as cell clusters. (B) Scanning electron micrographs of ancestral (left column) and evolved (right column) populations of the WT, monocultures of auxotrophs, and cocultures of auxotrophs during the early exponential growth phase. Scale bars: 5 μm.

(C) Growth of cocultured auxotrophs is contact-dependent. Cocultures of ancestral (striped boxes) and derived (blue boxes) auxotrophs were grown either together in the same compartment (– Filter) or separated by a filter membrane (+ Filter) that allows passage of free amino acids, but prevents direct, physical contact between bacterial cells. Letters indicate significant differences between groups (ANOVA followed by a Dunnett's T3 post hoc test: $p < 0.01$, $F = 49.473$, $df = 367$ (ancestral cocultures: n = 40, evolved cocultures: n = 144)).

only enhance an intercellular exchange of metabolites via diffusion [44] but might also generate positive fitness feedbacks among cells [19] that ultimately could explain the spread of cooperative phenotypes. To test the propensity of the derived populations of the three different experimental groups to form multicellular clusters, the size distribution of cellular aggregates within populations was analyzed during the exponential growth phase by laser diffraction spectroscopy. This experiment uncovered that in derived auxotrophic cocultures, the majority of cells (i.e., between 68 and 97% of all cells) existed within clusters of an average diameter of 45 μm. In contrast, populations of both derived WT and monocultures of auxotrophs were almost exclusively present in a unicellular form (Figure 3A).

In order to clarify whether cluster formation is a derived trait that emerged during the evolution experiment or a property that generally characterizes auxotrophic genotypes, the degree of cluster formation was compared between ancestral and derived consortia of auxotrophic genotypes. Analyzing an early time-point during the growth cycle of the two groups, at which cells were in their exponential growth phase (i.e., 8 h), revealed extensive cluster formation in both cases: the majority of cells (ca. 90%) were part of clusters (Figure S4A). This result indicates cluster formation did not evolve *de novo* but was already present in ancestral auxotrophs.

The same patterns were detected when cultures of ancestral and derived populations were visualized by scanning electron microscopy (Figure 3B). Also here, cluster formation was observed in both ancestral and derived populations of cocultured auxotrophs, whereas control populations consisted exclusively of individual cells. Interestingly, when pairs of coevolved auxotrophs were labeled with green or red fluorescent proteins and the resulting cocultures were imaged by fluorescence microscopy, cells within the observed clusters frequently displayed two fluorescent colors simultaneously (Figure S4B). This observation suggests an intercellular transport of cytoplasmic materials such as proteins and amino acids via, for example, intercellular nanotubes [34]. Together, these results show that in coculture, both ancestral and derived auxotrophic genotypes formed multicellular clusters.

Growth of Auxotrophic Cocultures Is Contact-Dependent

The prevalence of multicellular aggregates in all cocultures suggested this behavior is advantageous for auxotrophic mutants.

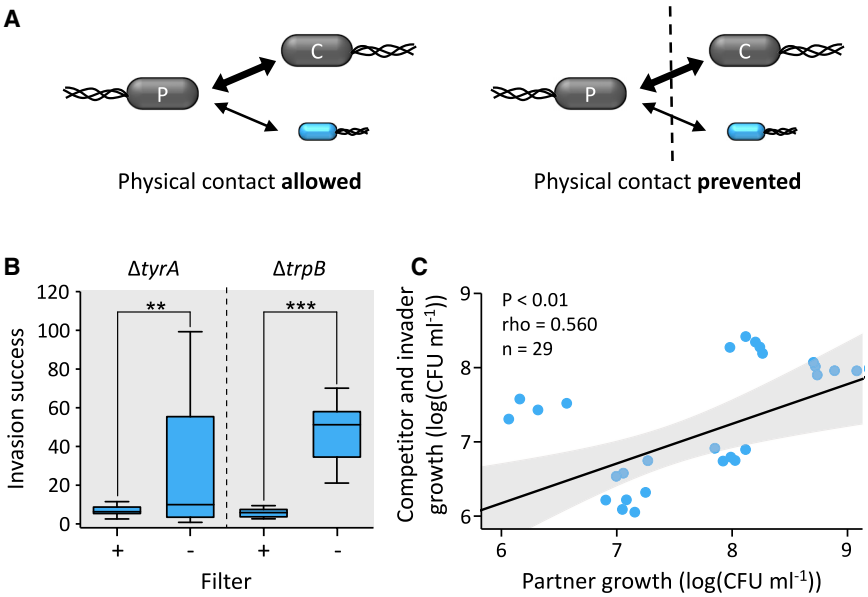

Figure 4. Positive Fitness Feedbacks within Multicellular Clusters Favor Cooperative Genotypes

(A) Experimental design. The ability of derived, cooperative auxotrophs (blue cell) to invade a population of ancestral, non-cooperative auxotrophs (gray cells, initial ratio: 1:1) from rare (20:1) was probed. For this, three consortia, each consisting of a tryptophan-auxotrophic (Δ*trpB*) or a tyrosine-auxotrophic genotype (Δ*tyrA*) were used. The invader (blue cell) and its ancestral competitor sharing the same auxotrophy (gray cell, C) competed for the focal amino acid produced by the ancestral partner genotype (gray cell, P) either in the absence (left) or presence of a filter membrane (right) that prevented a physical contact among cells.

(B) Invasion success of coevolved auxotrophs is significantly increased when cells can form clusters. Shown is the invasion success (i.e., net growth of invader relative to net growth of competitor over 72 h) per generation of derived, coevolved strains that are auxotrophic for tyrosine (Δ*tyrA*) or tryptophan (Δ*trpB*). Asterisks indicate significant differences (Wilcoxon signed ranks test: **$p < 0.01$, $Z = -2.613$, $n = 15$; ***$p < 0.001$, $Z = -3.408$, $n = 15$) between populations grown in the presence (+ Filter, i.e., cluster formation prevented) and absence of a filter membrane (− Filter, i.e., cluster formation allowed).

(C) Cluster formation results in positive fitness feedbacks among auxotrophic subpopulations. Net growth of the ancestral competitor + derived invader (y axis) and the ancestral partner (x axis) is significantly positively correlated when cells form clusters. A linear regression was fitted to the data (black line; grey area: ±95% confidence interval). The results of a Spearman rank correlation are shown.

See also Figure S5.

One likely explanation for this is that the spatial proximity, per se, allows auxotrophic genotypes to exchange essential amino acids more efficiently. To test this hypothesis, both ancestral and derived pairs of auxotrophic genotypes were grown in a device that allows cultivating both populations either together in the same compartment or separated by filter membrane (i.e., Nurmikko cells). The introduced filter membranes permit passage of free amino acids in the culture medium, but prevent any physical contact between bacterial cells [34]. Indeed, separating interaction partners in this way significantly reduced growth in both ancestral and evolved cocultures, thus confirming that physical contact between cells was key for an efficient transfer of amino acids between cells (Figure 3C). The fact that introducing the filter membrane affected the net growth of derived consortia less strongly than the ancestral consortium implies derived clones feature adaptations that make them less dependent on a very close physical contact with their partner strain. This could, for example, include an increased liberation of amino acids into the extracellular environment in derived but not the ancestral consortia. Together, this experiment confirmed that a close proximity among aggregated cells was necessary—particularly during early stages of the evolution experiment.

Positive Feedback Loops Favor Cooperation within Multicellular Clusters

Finally, we asked which evolutionary mechanism facilitated the observed evolution and maintenance of metabolic cooperation. Given that in all replicates analyzed, auxotrophic cells assembled into multicellular clusters (Figures 3A and 3B) and that these clusters were key to an efficient growth of auxotrophs (Figure 3C), we hypothesized that positive fitness feedbacks within multicellular clusters have benefitted cooperative cells. In contrast, individual cells outside of clusters should not be able to take advantage of this effect and thus experience a fitness disadvantage.

To test this hypothesis, we designed and performed an invasion-from-rare experiment that mimicked the emergence of a cooperative phenotype within a coculture of otherwise non-cooperative auxotrophs during the early phases of the evolution experiment. Under these conditions, a newly evolved cooperator (i.e., the "invader") is initially rare in frequency and competes with its evolutionary ancestor, which is common and shares the same auxotrophy (i.e., the "competitor") for the amino acids that are produced by the respective other auxotrophic strain (i.e., the "partner"). Importantly, both the competitor and the partner feature ancestral amino acid production levels. To evaluate the advantage that is gained by interacting within multicellular clusters, cooperators and their respective competitors were either cocultured together with the partner in the same environment or, alternatively, separated with a filter membrane, thus inhibiting cluster formation (Figure 4A). If positive fitness feedbacks operate on cooperative cells when being part of a cluster, the invasion success of cooperative auxotrophs should be high in the absence but low in the presence of the filter membrane. For this experiment, six cooperative phenotypes, which have been isolated from different evolved cocultures, were used as invaders (Figure 4B). In parallel, the invasion success of the corresponding ancestors of selected phenotypes was also determined in the presence of the filter (Figures S5A and S5B). Because in these experiments the invader and the competitor were the exact same genotype just inoculated in a different ratio, this setup allowed for

quantification of the basal invasion success of non-cooperative cells outside of clusters.

Analyzing the invasion success of ancestral and derived auxotrophic mutants in the presence of the filter membrane revealed basal invasion levels that did not differ between the two Tyr auxotrophs (Mann-Whitney U test: $p > 0.05$, $Z = -0.390$, $n = 25$), but marginally increased in case of the Trp auxotrophic mutants (Mann-Whitney U test: $p = 0.002$, $Z = -3.007$, $n = 30$; Figure S5B). The observation that the invasion success of Trp auxotrophic mutants increased over the course of the evolution experiment even when cells were not allowed to form clusters suggests these auxotrophic mutants have acquired an improved ability to grow under the nutrient-limiting conditions of the experiment.

Comparing the invasion success of derived coevolved auxotrophs in the absence and presence of the filter membrane revealed that in the absence of the filter, evolved cooperating types strongly increased in frequency and that this invasion success was significantly reduced when the two competing auxotrophs were physically separated from their respective partner by introducing a filter membrane (Wilcoxon signed ranks test: Δ*tyrA*: $p = 0.009$, $Z = -2.613$, $n = 15$; Δ*trpB*: $p = 0.001$, $Z = -3.408$, $n = 15$; Figure 4B). Some invaders achieved a 6-fold (Δ*tyrA*) or even 25-fold (Δ*trpB*) increase in frequency per generation and finally reached similar frequencies as their competitor, thus pointing to a tremendous selective advantage resulting from metabolic cooperation. Control experiments, in which the three-partite consortia were analyzed by laser diffraction spectroscopy, confirmed in all cases that cells formed multicellular clusters when they were cultivated without filter membranes (Figure S5C). Finally, to clarify whether an increased cooperative investment also benefitted the corresponding receiving cells, the statistical relationship between the growth of competitor and invader that both carry the same auxotrophy-causing mutation with the growth of partner cells carrying the complementary auxotrophy was determined. Both parameters showed a strongly positive and significant correlation in the absence (Spearman rank correlation: $p < 0.01$, $rho = 0.56$, $n = 29$; Figure 4C) but not in the presence of the filter membrane (Spearman rank correlation: $p = 0.957$, $rho = 0.012$, $n = 23$), thus providing direct experimental evidence for a positive feedback loop operating between both bacterial subpopulations.

Taken together, these results show that despite significant fitness costs, cooperative types gained a strong fitness advantage over non-cooperative auxotrophs when they were part of a multicellular cluster.

Both Amino Acid Overproduction and Cluster Formation Are Necessary for Cooperation to Evolve

Our empirical results suggested that positive fitness feedbacks among interacting genotypes drove the evolution of metabolic cooperation in our evolution experiment. Specifically, reciprocal cross-feeding interactions among two different auxotrophic genotypes evolved an increased cooperative investment into the corresponding partner when they were part of a multicellular cluster but not when they existed in isolation. To test the plausibility of this interpretation and independently vary the underlying parameters, a theoretical model was developed to identify the set of conditions favoring the evolution of mutualistic cooperation. This model describes the population dynamics of individual cells and cells in clusters, which form by aggregation of individual cells. Mutations arising with a certain frequency increase the production level of the traded commodity at a cost to the cell, thus giving rise to a cooperative mutant.

Analyzing the effect of both cluster formation and amino acid overproduction on the evolution of cooperation clearly revealed that both the formation of multicellular clusters and synergistic interactions among interaction partners within clusters were key for a costly metabolic cooperation to evolve (Figure 5). Reducing the values of either parameter drastically reduced the propensity, with which cooperative alleles in the population increased in frequency. In contrast, and in line with the experimental results, when cluster formation and amino acid production was high, cooperation evolved rapidly (Figure 5). Thus, this theoretical analysis suggests that cooperation emerges automatically because of positive fitness feedbacks when two genotypes (1) engage in an interaction that is mutually beneficial and (2) form spatially structured cell clusters.

DISCUSSION

The evolution of cooperation within populations of well-mixed bacteria poses a major problem for evolutionary biology [10–12]: why should individuals start to invest costly resources to benefit other bacteria rather than utilize these resources to maximize their own fitness? For these situations, evolutionary theory predicts that newly emerged genotypes that pay a cost for performing a cooperative behavior, but are not receiving any direct or indirect fitness benefits for this investment in return, should be selected against and thus be lost from a given population [13, 45]. Here, we show both theoretically and experimentally that cooperative cross-feeding of essential metabolites can rapidly evolve in populations of bacteria, whose growth requires a reciprocal exchange of essential metabolites among two bacterial genotypes. The transition from the initial byproduct interaction into a costly cooperation was due to the formation of multicellular clusters among bacteria. These structures not only enhanced the exchange of metabolites between cells in a well-mixed environment but also resulted in positive fitness feedbacks that benefitted cooperative mutants when being part of a multicellular cluster.

Spatial structuring has been previously suggested to facilitate the evolution and maintenance of cooperative interactions [16, 46–51]. Several causal reasons can account for this phenomenon. First, surface colonization of randomly mixed cooperative and non-cooperative genotypes results in local patches that differ in their genotypic composition. In areas were multiple cooperative genotypes colocalize by chance, cells can grow more than in patches, which are dominated by non-cooperators [51, 52]. Second, if cooperation is based on an exchange of metabolites, released compounds may locally accumulate and, as a consequence, preferentially benefit resident cells [51]. If the interaction lasts long enough, non-cooperating beneficiaries may then even start to cooperate by increasing the production of the exchanged metabolite themselves [48]. Third, as cells grow, self-organization within expanding populations can lead to a segregation of cooperative and non-cooperative cells,

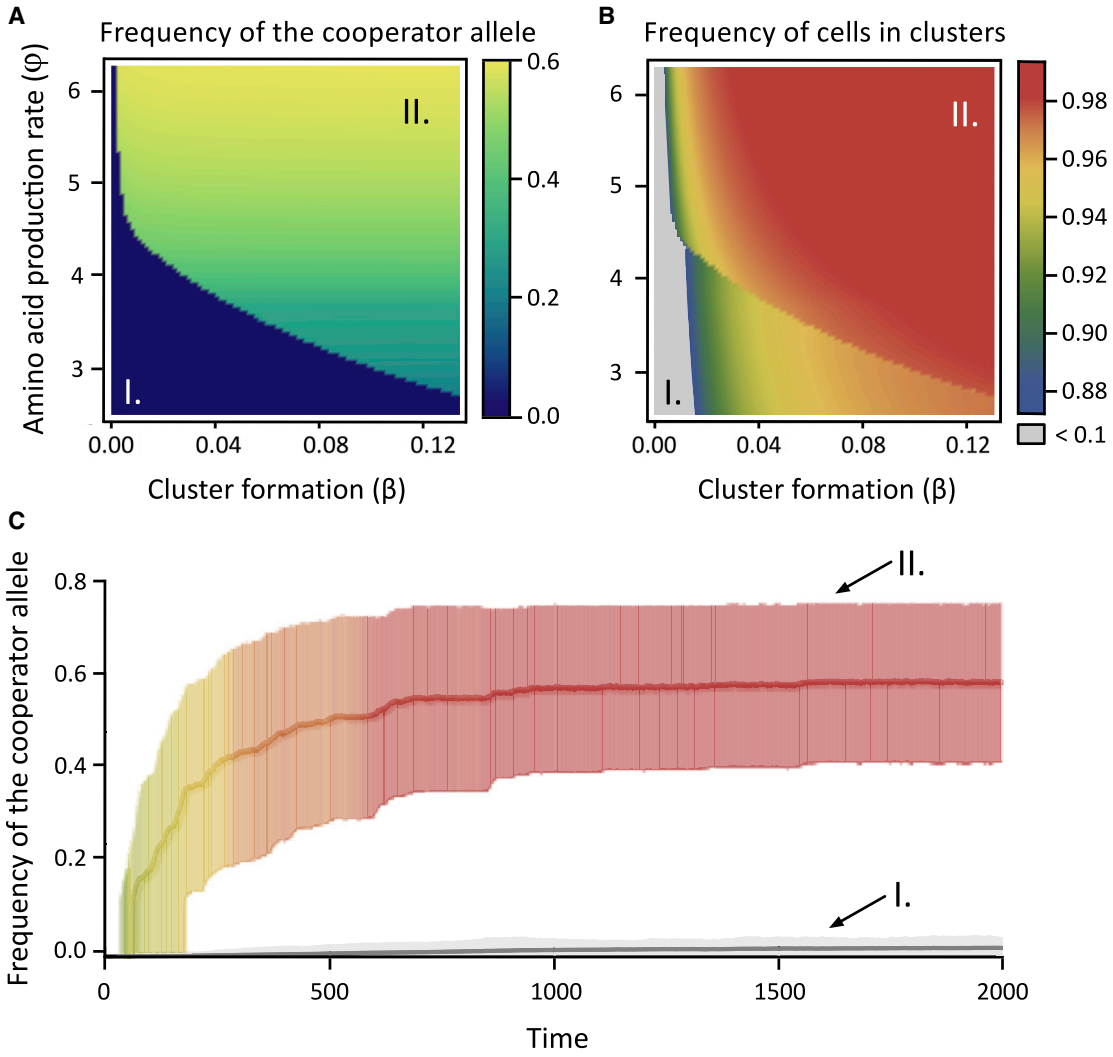

Figure 5. Evolution of Metabolic Cooperation Requires Both Spatial Clustering and an Increased Production of the Exchanged Metabolites

Shown are the results of a theoretical model that was developed to identify the causal parameters explaining the evolution of cooperation in our model system.

(A) Cooperation is favored when both amino acid production and cluster formation are high. The frequency of the cooperator allele in a population is displayed as a function of amino acid production and the rate of cluster formation.

(B) Cluster formation is prevalent, but particularly favored when amino acid production rates are high. The frequency of cells in clusters is plotted as a function of amino acid production and the rate of cluster formation.

(C) Cooperation evolves when cluster formation and amino acid production is high. Evolutionary dynamics of the cooperator allele under conditions shown in (A) and (B), where the degree of both amino acid production and cluster formation is low (I) or high (II). The mean frequency of the cooperator allele in a population (± confidence interval) of 100 replicates is shown. Color code of the line represents the frequency of cells in clusters according to (B).

See also Table S1 and S2.

thus resulting in a spatial exclusion of non-cooperators from cooperative benefits [51, 52]. However, even though it is known that bacteria can detach from colonized surfaces [53], it remains generally unclear how an increased productivity of more cooperative patches can be exported to the next generation of bacteria. Our work resolves this issue by showing that even in spatially unstructured environments, cooperation can evolve and persist for extended periods of time. The key criteria for this to happen is that bacteria generate a spatial structure that is independent of a surface-attached growth (Figure 3). By forming free-floating, multicellular aggregates, similar principles as outlined above for surface-attached communities apply. Indeed, the invasion-from-rare experiment strongly suggests local fitness feedbacks operate within multicellular clusters, which can explain the observed evolution of cooperation (Figures 4 and 5). Newly emerged mutants that increase their cooperative investment immediately benefit when they are part of a multicellular cluster (Figure 4). This effect is much stronger than a potentially detrimental effect of non-cooperating individuals. In fact, our results show that due to the formation of multicellular clusters, non-cooperating genotypes were significantly less fit than cooperating cells. This mechanism can explain the evolutionary transition from an interaction, in which metabolic byproducts are reciprocally exchanged, to a cooperative mutualism, in which both

parties evolved a costly overproduction of metabolites to benefit their corresponding partner.

Interestingly, the formation of multicellular aggregates was not a derived trait but characterized already ancestral cocultures of auxotrophs (Figures 3A, 3B, and S4A). Under our experimental conditions, auxotrophic cells could only grow when they derived amino acids from other cells in their environment. By physically attaching to each other, the spatial distance between donor and recipient cells is reduced, which likely facilitates an exchange of metabolites between cells [38, 54]. However, what triggered the formation of multicellular aggregates? One likely explanation is a physiological stress response that resulted from the starvation of auxotrophs for the two amino acids (Figure 3B). In our experimental setup, auxotrophs that were grown in cocultures most likely experienced phases of severe amino acid deprivation, while this was not (or to a lesser extent) the case for monocultures of amino acid-supplemented auxotrophs as well as for populations of prototrophic WT cells. Starvation for amino acids is known to trigger the so-called stringent response in auxotrophic bacteria [55], which upregulates the production of fimbriae [56] or extracellular polymeric substances [57] leading to autoaggregation [58]. An alternative mechanism could be the formation of intercellular nanotubes that is also induced by amino acid starvation in auxotrophic bacteria [34, 42]. The detection of double-labeled cells in cocultures of auxotrophic genotypes (Figure S4B) corroborates that auxotrophic cells exchanged cytoplasmic materials—most likely via nanotubes. The absence of a starvation response in amino acid-supplemented monocultures of auxotrophs as well as in populations of the prototrophic WT can likely explain the lack of aggregation in these experimental groups.

The results of our study are also relevant to other mutualistic interactions, in which two partners reciprocally exchange synergistic benefits. Very often, these interactions are strongly localized and rely on a physical contact between partners, which is conceptually equivalent to the formation of clusters observed in our study. Reciprocity has been previously suggested as an important mechanism contributing to the long-term maintenance of these mutualistic interactions [59]. In addition, the observation that experimentally reducing the mutualistic service provided by one partner also negatively impacted its growth was interpreted as a sanctioning behavior of the respective other individual to penalize its less-cooperative partner [60]. Other studies, in which interactions with more or less cooperative partners were compared, revealed that more cooperative partners benefitted by also receiving more resources in return [61, 62]. However, the patterns observed in these interspecific mutualisms are consistent with the positive fitness feedback described here. By locally assembling individuals that reciprocally exchange benefits, cooperation can be strongly favored (Figures 4 and 5). This explanation does not require derived mechanisms to quantify the investment of a partner and launch a corresponding response. Instead, positive fitness feedbacks that emerge automatically from reciprocal interactions in spatially structured communities are sufficient to account for the evolution and maintenance of these cooperative interactions.

Our experiment was initiated with a coculture of two auxotrophic genotypes, whose growth depended on a reciprocal exchange of essential amino acids. This situation is likely common in natural bacterial communities. Here, nutrient levels are frequently low, which typically results in stress responses such as the formation of surface-attached or free-floating biofilms [36]. Similar to the clusters observed in our study, these multicellular aggregates also facilitate an exchange of metabolites among cells [63–66]. In addition, sequencing data suggest auxotrophic bacteria are generally common in natural microbial communities [67]. Combining these two observations with the data presented here suggests similar evolutionary dynamics as observed in our study are likely common in natural microbial communities. Future work should identify whether this is indeed the case and which factors promote or hamper the type of synergistic coevolution observed in this study.

Taken together, the results presented in this work show how simple changes in the genomes of bacteria, in this case the loss of two biosynthetic genes, can set off an evolutionary dynamic that drastically reconfigures the ecology and evolution of the entire microbial community. The fact that these mutations forced the two resulting strains to interact with each other in order to grow paved the way for the initial byproduct interaction to evolve into a truly cooperative and costly metabolic interaction. Key factors driving this change were (1) the assortment of auxotrophic bacteria into multicellular clusters and (2) positive fitness feedbacks that operated on cells within these clusters, which favored cooperative mutants. Given the prevalence of auxotrophic bacteria in natural microbial communities [67], and the ease with which cooperative interactions evolve between those auxotrophs (this study), it is likely that cooperative metabolic interactions may be much more common than previously thought.

STAR★METHODS

Detailed methods are provided in the online version of this paper and include the following:

- KEY RESOURCES TABLE
- RESOURCE AVAILABILITY
  - Lead Contact
  - Materials Availability
  - Data and Code Availability
- EXPERIMENTAL MODEL AND SUBJECT DETAILS
  - Strain construction
- METHOD DETAILS
  - Culture conditions and general procedures
  - Evolution experiment
  - Relative fitness of ancestral versus evolved populations
  - Quantification of amino acid production levels using biosensors
  - Cost of adaptation
  - Contact-dependent growth
  - Cluster formation
  - Scanning electron microscopy
  - Invasion-from-rare experiment
  - Population dynamic model
- QUANTIFICATION AND STATISTICAL ANALYSIS
  - Relative fitness
  - Amino acid production levels
  - Invasion success
  - Statistical analysis

SUPPLEMENTAL INFORMATION

Supplemental Information can be found online at https://doi.org/10.1016/j.cub.2020.06.100.

A video abstract is available at https://doi.org/10.1016/j.cub.2020.06.100#mmc3.

ACKNOWLEDGMENTS

We thank Martin Kaltenpoth and his research group, Will Ratcliff, Paul Rainey, Ákos Kovács, Christoph Kaleta, Karin Frank, and the entire Kostlab (present and past) for useful discussion as well as three anonymous reviewers for constructive criticism on earlier versions of the manuscript. Help by Daniel Veit and Frank Mueller with manufacturing the Nurmikko cells, technical assistance by Marita Hermann with fitness and invasion-from-rare experiments, as well as support by Katherina Psathaki and Britta Brickwedde with SEM imaging is gratefully acknowledged. This research was supported by the Volkswagen Foundation (I/85 290: C.K.), the Jena School for Microbial Communication (C.K. and D.P.), the German Research Foundation (SFB 944, P19: C.K. and D.P.; SPP1617, KO 3909/2-1: C.K. and S.G.), and the University of Osnabrück (L.O.; EvoCell: C.K. and L.K.M.).

AUTHOR CONTRIBUTIONS

Conceptualization, C.K. and D.P.; Methodology, C.K., D.P., S.G., L.K.M., and L.O.; Formal Analysis, D.P., S.G., L.O., and L.K.M., Investigation, D.P., S.G., L.K.M., and L.O.; Resources, C.K.; Writing – Original Draft, D.P. and C.K.; Writing – Review & Editing, C.K., S.G., L.K.M., and L.O.; Visualization, D.P., S.G., L.K.M., L.O., and C.K.; Supervision, Project Administration, and Funding Acquisition, C.K.

DECLARATION OF INTERESTS

The authors declare no competing interests.

Received: January 10, 2020
Revised: April 29, 2020
Accepted: June 29, 2020
Published: July 23, 2020

REFERENCES

1. Boucher, D.H. (1988). The biology of mutualism: Ecology and evolution (New York: Oxford University Press).
2. J.L. Bronstein, ed. (2015). Mutualism (London: Oxford University Press).
3. Hodges, S.A., and Arnold, M.L. (1995). Spurring plant diversification: Are floral nectar spurs a key innovation? Proc. Biol. Sci. *262*, 343–348.
4. Janson, E.M., Stireman, J.O.I., 3rd, Singer, M.S., and Abbot, P. (2008). Phytophagous insect-microbe mutualisms and adaptive evolutionary diversification. Evolution *62*, 997–1012.
5. Sudakaran, S., Kost, C., and Kaltenpoth, M. (2017). Symbiont acquisition and replacement as a source of ecological innovation. Trends Microbiol. *25*, 375–390.
6. Litsios, G., Sims, C.A., Wüest, R.O., Pearman, P.B., Zimmermann, N.E., and Salamin, N. (2012). Mutualism with sea anemones triggered the adaptive radiation of clownfishes. BMC Evol. Biol. *12*, 212.
7. Seth, E.C., and Taga, M.E. (2014). Nutrient cross-feeding in the microbial world. Front. Microbiol. *5*, 350.
8. Ankrah, N.Y.D., and Douglas, A.E. (2018). Nutrient factories: metabolic function of beneficial microorganisms associated with insects. Environ. Microbiol. *20*, 2002–2011.
9. Morris, B.E., Henneberger, R., Huber, H., and Moissl-Eichinger, C. (2013). Microbial syntrophy: interaction for the common good. FEMS Microbiol. Rev. *37*, 384–406.
10. Hamilton, W.D. (1963). The evolution of altruistic behavior. Am. Nat. *97*, 354–356.
11. Hamilton, W.D. (1964). The genetical evolution of social behaviour. I. J. Theor. Biol. *7*, 1–16.
12. Hamilton, W.D. (1964). The genetical evolution of social behaviour. II. J. Theor. Biol. *7*, 17–52.
13. Nowak, M.A. (2006). Five rules for the evolution of cooperation. Science *314*, 1560–1563.
14. Sachs, J.L., and Simms, E.L. (2006). Pathways to mutualism breakdown. Trends Ecol. Evol. *21*, 585–592.
15. Ferriere, R., Bronstein, J.L., Rinaldi, S., Law, R., and Gauduchon, M. (2002). Cheating and the evolutionary stability of mutualisms. Proc. Biol. Sci. *269*, 773–780.
16. Germerodt, S., Bohl, K., Lück, A., Pande, S., Schröter, A., Kaleta, C., Schuster, S., and Kost, C. (2016). Pervasive selection for cooperative cross-feeding in bacterial communities. PLoS Comput. Biol. *12*, e1004986.
17. Frank, S.A. (1994). Genetics of mutualism: the evolution of altruism between species. J. Theor. Biol. *170*, 393–400.
18. Doebeli, M., and Knowlton, N. (1998). The evolution of interspecific mutualisms. Proc. Natl. Acad. Sci. USA *95*, 8676–8680.
19. Estrela, S., Kerr, B., and Morris, J.J. (2016). Transitions in individuality through symbiosis. Curr. Opin. Microbiol. *31*, 191–198.
20. Flemming, H.C., and Wuertz, S. (2019). Bacteria and archaea on Earth and their abundance in biofilms. Nat. Rev. Microbiol. *17*, 247–260.
21. Tolker-Nielsen, T., and Molin, S. (2000). Spatial organization of microbial biofilm communities. Microb. Ecol. *40*, 75–84.
22. Taylor, P.D. (1992). Altruism in viscous populations - an inclusive fitness model. Evol. Ecol. *6*, 352–356.
23. Wilson, D.S., Pollock, G.B., and Dugatkin, L.A. (1992). Can altruism evolve in purely viscous populations? Evol. Ecol. *6*, 331–341.
24. Queller, D. (1994). Genetic relatedness in viscous populations. Evol. Ecol. *8*, 70–73.
25. West, S.A., Murray, M.G., Machado, C.A., Griffin, A.S., and Herre, E.A. (2001). Testing Hamilton's rule with competition between relatives. Nature *409*, 510–513.
26. Macarthur, R., and Levins, R. (1964). Competition, habitat selection, and character displacement in a patchy environment. Proc. Natl. Acad. Sci. USA *51*, 1207–1210.
27. Estrela, S., and Brown, S.P. (2013). Metabolic and demographic feedbacks shape the emergent spatial structure and function of microbial communities. PLoS Comput. Biol. *9*, e1003398.
28. Hauert, C., and Doebeli, M. (2004). Spatial structure often inhibits the evolution of cooperation in the snowdrift game. Nature *428*, 643–646.
29. Frank, S.A. (1998). Foundations of social evolution (Princeton, New Jersey: Princeton University Press).
30. Mitri, S., Xavier, J.B., and Foster, K.R. (2011). Social evolution in multispecies biofilms. Proc. Natl. Acad. Sci. USA *108* (*Suppl 2*), 10839–10846.
31. Müller, M.J.I., Neugeboren, B.I., Nelson, D.R., and Murray, A.W. (2014). Genetic drift opposes mutualism during spatial population expansion. Proc. Natl. Acad. Sci. USA *111*, 1037–1042.
32. Oliveira, N.M., Niehus, R., and Foster, K.R. (2014). Evolutionary limits to cooperation in microbial communities. Proc. Natl. Acad. Sci. USA *111*, 17941–17946.
33. Benomar, S., Ranava, D., Cárdenas, M.L., Trably, E., Rafrafi, Y., Ducret, A., Hamelin, J., Lojou, E., Steyer, J.P., and Giudici-Orticoni, M.T. (2015). Nutritional stress induces exchange of cell material and energetic coupling between bacterial species. Nat. Commun. *6*, 6283.
34. Pande, S., Shitut, S., Freund, L., Westermann, M., Bertels, F., Colesie, C., Bischofs, I.B., and Kost, C. (2015). Metabolic cross-feeding via intercellular nanotubes among bacteria. Nat. Commun. *6*, 6238.
35. Cordero, O.X., and Datta, M.S. (2016). Microbial interactions and community assembly at microscales. Curr. Opin. Microbiol. *31*, 227–234.

36. Flemming, H.-C., Wingender, J., Szewzyk, U., Steinberg, P., Rice, S.A., and Kjelleberg, S. (2016). Biofilms: an emergent form of bacterial life. Nat. Rev. Microbiol. *14*, 563–575.

37. Laganenka, L., Colin, R., and Sourjik, V. (2016). Chemotaxis towards autoinducer 2 mediates autoaggregation in Escherichia coli. Nat. Commun. *7*, 12984.

38. Marchal, M., Goldschmidt, F., Derksen-Müller, S.N., Panke, S., Ackermann, M., and Johnson, D.R. (2017). A passive mutualistic interaction promotes the evolution of spatial structure within microbial populations. BMC Evol. Biol. *17*, 106.

39. Trunk, T., Khalil, H.S., and Leo, J.C. (2018). Bacterial autoaggregation. AIMS Microbiol *4*, 140–164.

40. Blank, D., Wolf, L., Ackermann, M., and Silander, O.K. (2014). The predictability of molecular evolution during functional innovation. Proc. Natl. Acad. Sci. USA *111*, 3044–3049.

41. D'Souza, G., Shitut, S., Preussger, D., Yousif, G., Waschina, S., and Kost, C. (2018). Ecology and evolution of metabolic cross-feeding interactions in bacteria. Nat. Prod. Rep. *35*, 455–488.

42. Shitut, S., Ahsendorf, T., Pande, S., Egbert, M., and Kost, C. (2019). Nanotube-mediated cross-feeding couples the metabolism of interacting bacterial cells. Environ. Microbiol. *21*, 1306–1320.

43. Bertels, F., Merker, H., and Kost, C. (2012). Design and characterization of auxotrophy-based amino acid biosensors. PLoS ONE *7*, e41349.

44. Weigert, M., and Kümmerli, R. (2017). The physical boundaries of public goods cooperation between surface-attached bacterial cells. Proc. Biol. Sci. *284*, 20170631.

45. West, S.A., Diggle, S.P., Buckling, A., Gardner, A., and Griffins, A.S. (2007). The social lives of microbes. Annu. Rev. Ecol. Evol. Syst. *38*, 53–77.

46. Bever, J.D., Richardson, S.C., Lawrence, B.M., Holmes, J., and Watson, M. (2009). Preferential allocation to beneficial symbiont with spatial structure maintains mycorrhizal mutualism. Ecol. Lett. *12*, 13–21.

47. Harcombe, W. (2010). Novel cooperation experimentally evolved between species. Evolution *64*, 2166–2172.

48. Harcombe, W.R., Chacón, J.M., Adamowicz, E.M., Chubiz, L.M., and Marx, C.J. (2018). Evolution of bidirectional costly mutualism from byproduct consumption. Proc. Natl. Acad. Sci. USA *115*, 12000–12004.

49. Werner, G.D.A., Strassmann, J.E., Ivens, A.B.F., Engelmoer, D.J.P., Verbruggen, E., Queller, D.C., Noë, R., Johnson, N.C., Hammerstein, P., and Kiers, E.T. (2014). Evolution of microbial markets. Proc. Natl. Acad. Sci. USA *111*, 1237–1244.

50. Yamamura, N., Higashi, M., Behera, N., and Yuichiro Wakano, J. (2004). Evolution of mutualism through spatial effects. J. Theor. Biol. *226*, 421–428.

51. Pande, S., Kaftan, F., Lang, S., Svatoš, A., Germerodt, S., and Kost, C. (2016). Privatization of cooperative benefits stabilizes mutualistic cross-feeding interactions in spatially structured environments. ISME J. *10*, 1413–1423.

52. Momeni, B., Waite, A.J., and Shou, W. (2013). Spatial self-organization favors heterotypic cooperation over cheating. eLife *2*, e00960.

53. Petrova, O.E., and Sauer, K. (2016). Escaping the biofilm in more than one way: desorption, detachment or dispersion. Curr. Opin. Microbiol. *30*, 67–78.

54. Christensen, B.B., Haagensen, J.A.J., Heydorn, A., and Molin, S. (2002). Metabolic commensalism and competition in a two-species microbial consortium. Appl. Environ. Microbiol. *68*, 2495–2502.

55. Traxler, M.F., Summers, S.M., Nguyen, H.T., Zacharia, V.M., Hightower, G.A., Smith, J.T., and Conway, T. (2008). The global, ppGpp-mediated stringent response to amino acid starvation in *Escherichia coli*. Mol. Microbiol. *68*, 1128–1148.

56. Kelly, A., Conway, C., O Cróinín, T., Smith, S.G.J., and Dorman, C.J. (2006). DNA supercoiling and the Lrp protein determine the directionality of fim switch DNA inversion in *Escherichia coli* K-12. J. Bacteriol. *188*, 5356–5363.

57. Costa, O.Y.A., Raaijmakers, J.M., and Kuramae, E.E. (2018). Microbial extracellular polymeric substances: Ecological function and impact on soil aggregation. Front. Microbiol. *9*, 1636.

58. Schembri, M.A., Christiansen, G., and Klemm, P. (2001). FimH-mediated autoaggregation of *Escherichia coli*. Mol. Microbiol. *41*, 1419–1430.

59. Trivers, R.L. (1971). The evolution of reciprocal altruism. Q. Rev. Biol. *46*, 35–57.

60. Kiers, E.T., Rousseau, R.A., West, S.A., and Denison, R.F. (2003). Host sanctions and the legume-rhizobium mutualism. Nature *425*, 78–81.

61. Kiers, E.T., Duhamel, M., Beesetty, Y., Mensah, J.A., Franken, O., Verbruggen, E., Fellbaum, C.R., Kowalchuk, G.A., Hart, M.M., Bago, A., et al. (2011). Reciprocal rewards stabilize cooperation in the mycorrhizal symbiosis. Science *333*, 880–882.

62. Simms, E.L., Taylor, D.L., Povich, J., Shefferson, R.P., Sachs, J.L., Urbina, M., and Tausczik, Y. (2006). An empirical test of partner choice mechanisms in a wild legume-rhizobium interaction. Proc. Biol. Sci. *273*, 77–81.

63. Jahn, U., Gallenberger, M., Paper, W., Junglas, B., Eisenreich, W., Stetter, K.O., Rachel, R., and Huber, H. (2008). *Nanoarchaeum equitans* and *Ignicoccus hospitalis*: new insights into a unique, intimate association of two archaea. J. Bacteriol. *190*, 1743–1750.

64. Summers, Z.M., Fogarty, H.E., Leang, C., Franks, A.E., Malvankar, N.S., and Lovley, D.R. (2010). Direct exchange of electrons within aggregates of an evolved syntrophic coculture of anaerobic bacteria. Science *330*, 1413–1415.

65. He, X., McLean, J.S., Edlund, A., Yooseph, S., Hall, A.P., Liu, S.Y., Dorrestein, P.C., Esquenazi, E., Hunter, R.C., Cheng, G., et al. (2015). Cultivation of a human-associated TM7 phylotype reveals a reduced genome and epibiotic parasitic lifestyle. Proc. Natl. Acad. Sci. USA *112*, 244–249.

66. Cerqueda-García, D., Martínez-Castilla, L.P., Falcón, L.I., and Delaye, L. (2014). Metabolic analysis of *Chlorobium chlorochromatii* CaD3 reveals clues of the symbiosis in '*Chlorochromatium aggregatum*'. ISME J. *8*, 991–998.

67. D'Souza, G., Waschina, S., Pande, S., Bohl, K., Kaleta, C., and Kost, C. (2014). Less is more: selective advantages can explain the prevalent loss of biosynthetic genes in bacteria. Evolution *68*, 2559–2570.

68. Baba, T., Ara, T., Hasegawa, M., Takai, Y., Okumura, Y., Baba, M., Datsenko, K.A., Tomita, M., Wanner, B.L., and Mori, H. (2006). Construction of Escherichia coli K-12 in-frame, single-gene knockout mutants: The Keio collection. Mol. Syst. Biol. *2*, 2006.0008.

69. Lenski, R.E., Rose, M.R., Simpson, S.C., and Tadler, S.C. (1991). Long-term experimental evolution in *Escherichia coli*. I. Adaptation and divergence during 2,000 generations. Am. Nat. *138*, 1315–1341.

70. Blattner, F.R., Plunkett, G., 3rd, Bloch, C.A., Perna, N.T., Burland, V., Riley, M., Collado-Vides, J., Glasner, J.D., Rode, C.K., Mayhew, G.F., et al. (1997). The complete genome sequence of *Escherichia coli* K-12. Science *277*, 1453–1462.

71. Datsenko, K.A., and Wanner, B.L. (2000). One-step inactivation of chromosomal genes in *Escherichia coli* K-12 using PCR products. Proc. Natl. Acad. Sci. USA *97*, 6640–6645.

72. Rasband, W.S. (2018). ImageJ (U. S. National Institutes of Health). https://imagej.nih.gov/ij/.

73. Thomason, L.C., Costantino, N., and Court, D.L. (2007). E. coli genome manipulation by P1 transduction. Curr. Protoc. Mol. Biol. https://doi.org/10.1002/0471142727.mb0117s79.

74. Levin, B.R., Stewart, F.M., and Chao, L. (1977). Resource-limited growth, competition, and predation: A model and experimental studies with bacteria and bacteriophage. Am. Nat. *111*, 3–24.

75. Vanstockem, M., Michiels, K., Vanderleyden, J., and Van Gool, A.P. (1987). Transposon mutagenesis of *Azospirillum brasilense* and *Azospirillum lipoferum*: Physical analysis of Tn5 and Tn5-Mob insertion mutants. Appl. Environ. Microbiol. *53*, 410–415.

STAR★METHODS

KEY RESOURCES TABLE

REAGENT or RESOURCE	SOURCE	IDENTIFIER
Chemicals		
Lysogeny broth (LB), Lennox	Carl Roth GmbH	Catalog # X964.1
Agar-Agar Kobe	Carl Roth GmbH	Catalog # 5210.2
Dipotassium hydrogen phosphate	Carl Roth GmbH	Catalog # 26931.263
Sodium dihydrogen phosphate	Carl Roth GmbH	Catalog # T879.2
Magnesium sulfate heptahydrate	Carl Roth GmbH	Catalog # P027.2
Potassium chloride	VWR	Catalog # 26764.260
Calcium chloride dihydrate	Carl Roth GmbH	Catalog # 5239.2
Ammonium chloride	VWR	Catalog # 21236.267
Iron (II) sulfate heptahydrate	Merck	Catalog # 3965
Glucose	Carl Roth GmbH	Catalog # 6887.1
Kanamycin	Carl Roth GmbH	Catalog # T832.2
Chloramphenicol	Carl Roth GmbH	Catalog # 3886.1
Ampicillin sodium salt	Carl Roth GmbH	Catalog # K029.2
IPTG (Isopropyl β-D-1-thiogalactopyranoside)	Carl Roth GmbH	Catalog # 2316.4
X-Gal (5-bromo-4-chloro-3-indolyl-β-D-galactopyranoside)	Carl Roth GmbH	Catalog # 3215.4
TTC (tetrazolium chloride)	Sigma	Catalog # T8877
Arabinose	Carl Roth GmbH	Catalog # 5118.2
Glycerol	Carl Roth GmbH	Catalog # 3783.1
L-Tryptophan	AppliChem	Catalog # A3445
L-Tyrosine disodium salt	AppliChem	Catalog # A2838
Experimental Models: Organisms/Strains		
Escherichia coli BW25113 ara$^-$, lacZ$^-$	[68]	N/A
Escherichia coli BW25113 ara$^+$, lacZ$^+$	This study	N/A
Escherichia coli BW25113 ara$^-$, lacZ$^-$, Δ*trpB::kan*^{R}	This study	N/A
Escherichia coli BW25113 ara$^-$, lacZ$^-$, Δ*tyrA::kan*^{R}	This study	N/A
Escherichia coli BW25113 ara$^+$, lacZ$^+$, Δ*trpB::kan*^{R}	This study	N/A
Escherichia coli BW25113 ara$^+$, lacZ$^+$, Δ*tyrA::kan*^{R}	This study	N/A
Escherichia coli REL607	[69]	N/A
Escherichia coli MG1655	[70]	N/A
Recombinant DNA		
pKD3	[71]	N/A
pKD46	[71]	N/A
pJBA24-*egfp*	[43]	N/A
pJBA24-*mCherry*	[34]	N/A
Software and Algorithms		
Origin Pro 2017	OriginLab, Northampton, MA	N/A
IBM SPSS statistics 26	Version 26.0., released 2019, IBM Corp., SPSS Statistics, Armonk, NY.	N/A
ImageJ	[72]	https://imagej.nih.gov/ij/
Magellan	Version 7.1, Tecan Group Ltd., Switzerland	N/A
Mathematica	N/A	https://www.wolfram.com/mathematica/

RESOURCE AVAILABILITY

Lead Contact

Further information and requests for resources should be directed to and will be fulfilled by the Lead Contact, Christian Kost (christiankost@gmail.com).

Materials Availability

This study did not generate new unique reagents.

Data and Code Availability

The datasets supporting the current study are available from the Lead Contact on request. This study did not generate any code.

EXPERIMENTAL MODEL AND SUBJECT DETAILS

Strain construction

To synthetically design an obligate cross-feeding interaction that was based on a reciprocal exchange of essential amino acids, *Escherichia coli* BW25113 [68] was used as wild type (WT). Cells were genetically modified by P1 transduction [73] to generate in-frame knockout mutants by the replacement of target genes with a kanamycin resistance cassette [68, 71]. The resulting mutants lacked the genes *tyrA* or *trpB* that encode enzymes responsible for the terminal amino acid biosynthesis step of tyrosine or tryptophan, respectively. To allow phenotypic discrimination of these two auxotrophic genotypes on agar plates, the marker genes *araDAB* (derived from *E. coli* REL607 [69]) and the functional *lacZ*-gene (derived from *E. coli* MG1655 [70]) were additionally introduced by P1 transduction. As a result, strains carrying the functional alleles for arabinose utilization and β-galactosidase appear blue on modified TA-agar [74] that additionally contained 0.1 mM IPTG (Isopropyl β-D-1-thiogalactopyranoside) and 50 μg ml^{-1} x-Gal (5-bromo-4-chloro-3-indolyl-β-D-galactopyranoside), while the WT phenotype appears red. The presence of the resistance cassette, the marker genes, and the amino acid auxotrophy was first confirmed by plating on selective agar plates and further verified by whole genome re-sequencing.

To determine amino acid production rates of a donor genotype, amino acid biosensors were generated to quantify the amount of tyrosine and tryptophan produced by donor cells [43]. The corresponding genotypes carried the functional *lacZ*-gene and had either the *trpB* or *tyrA* deleted from their genome as described above. The resulting genotypes *E. coli* Δ*trpB::kan lacZ* and *E. coli* Δ*tyrA::kan lacZ* were further modified to enable quantification of colony forming units (CFU) on agar plates, even when present in low frequencies. For this, the kanamycin resistance cassette was replaced with a chloramphenicol resistance cassette [71]. In detail, the chloramphenicol cassette (*camR* gene) from pKD3 was amplified by PCR using the reported primers for both FRT sites that direct site-specific recombination. After transforming the λ Red helper plasmid pKD46 into both genotypes, electroporation with the PCR-product was performed [71]. Generated constructs containing *camR* were selected on LB agar containing 30 μg ml^{-1} chloramphenicol and restored sensitivity for kanamycin was confirmed.

Plasmids pJBA24-*egfp* [43] or pJBA24-*mCherry* [34] that constitutively express the green (eGFP) or red (mCherry) fluorescent protein as well as a β-lactamase were transformed into all derived auxotrophic genotypes that have been isolated from one of the derived populations.

METHOD DETAILS

Culture conditions and general procedures

In all experiments, cells were grown using minimal medium for *Azospirillium brasilense* (MMAB) [75] without biotin using 0.5% glucose instead of malate as a carbon source. To obtain MMAB agar, two-fold concentrated Kobe-agar (30 g l^{-1}) was added to 2-fold concentrated MMAB medium in a 1:1 ratio. Unless otherwise noted, culture conditions were kept constant between experiments (30°C, 225 rpm) and precultures of auxotrophic genotypes were supplemented with amino acid (150 μM tyrosine or tryptophan, respectively). If not indicated otherwise, these amino acid concentrations were generally used for supplementation. Bacterial strains were freshly streaked on LB agar and incubated for 24 h or until single colonies showed sufficient size for inoculation of liquid cultures. Individual colonies were used as biological replicates to inoculate 1 mL overnight precultures in 96 deep-well plates (max. volume: 2 ml, Thermo Scientific Nunc), which were diluted to an optical density at 600 nm (OD_{600nm}) of 0.1 the next day. Unless otherwise specified, these precultures were used to inoculate 1 mL MMAB medium with a final OD_{600nm} of 0.001. To enable blue-white screening of colonies, 0.1 mM IPTG and 50 μg ml^{-1} x-Gal was added to the agar. Antibiotics were used at the following concentrations: kanamycin 50 μg ml^{-1} and chloramphenicol 30 μg ml^{-1}.

Evolution experiment

The evolution experiment consisted of three main experimental groups: (1) monocultures of *E. coli* WT that were cultivated in unsupplemented minimal medium, (2) monocultures of auxotrophs (i.e., either Δ*tyrA* or Δ*trpB*) that were cultivated in minimal medium containing Tyr or Trp in non-saturating concentrations (i.e., 50 μM), or (3) cocultures of auxotrophic genotypes (Δ*tyrA* + Δ*trpB*) that were

cultivated in unsupplemented minimal medium (Figure 1A). To generate the synthetically designed obligate byproduct interaction, complementary phenotypes (*i.e., E. coli* Tyr$^-$ Ara$^+$ Lac$^+$ & *E. coli* Trp$^-$ Ara$^-$ Lac$^-$ or the reverse combination of phenotypic labeling and auxotrophy) were combined in cocultures in an initial 1:1 ratio. Six biological replicates of each genotype (i.e., WT, Δ*tyrA*, and Δ*trpB* either with or without both phenotypic markers) were used to start the evolution experiment, adding up to 12 WT monocultures, 24 monocultures of auxotrophs, and 12 cocultures of auxotrophs. Besides differences in the culture medium, all populations were treated in an identical way during the evolution experiment.

The evolution experiment was initiated by reviving all genotypes from permanent cultures that were stored at −80°C. For this, stock cultures were directly inoculated into 4 mL of minimal medium (WT) or 4 mL of minimal medium that contained 150 μM of one of the two amino acids (auxotrophs). After 24 h of growth at 30°C, these cultures were plated on agar plates containing the same medium as before in its solidified form. After incubation of these plates for 48 h at 30°C, individual colonies of each genotype were picked and inoculated into a preculture using the same medium and culture conditions as before. The next day, the evolution experiment was started by inoculating 4 mL of minimal medium into 20 mL scintillation vials (Wheaton Industries Inc., USA) with an initial OD_{600nm} of 0.005. Always two precultures of auxotrophs (Δ*tyrA* and Δ*trpB*) were used to inoculate two monocultures of auxotrophs and one coculture of auxotrophs. Since these samples originated from the same two colonies, they were considered as matched pairs in subsequent experiments. Populations were initially transferred every seven days for a total of five transfers, following 15 transfers every three days, adding up to a total of 80 days or approximately 150 generations of bacterial growth. At the end of each cycle, optical densities were determined at 600 nm via spectrophotometry in a plate reader (Spectramax M5, Applied Biosystems). To disrupt any bacterial aggregate that might have formed during growth, populations were vortexed for one minute to separate cells. Subsequent tests with a representative number of samples using microscopy and laser diffractometry (see below) confirmed that this procedure successfully disrupted multicellular clusters. 20 μl of each culture were transferred into 4 mL of fresh MMAB medium. Depending on the length of the cycle (i.e., three or seven days), glycerol stocks (20% glycerol) were prepared every six or seven days and stored at −80°C. Cocultures were regularly tested for revertant phenotypes that showed prototrophic growth (i.e., that were capable to grow on MMAB agar without amino acid supplementation). Out of twelve cocultures, two were excluded from further analysis due to the detection of prototrophic phenotypes. Accordingly, also the two cognate replicates of auxotrophic monocultures were excluded from further analysis.

In addition, one replicate of the monocultures of auxotrophs (i.e., *E. coli* Δ*tyrA* Δ*araDAB* Δ*lacZ*) was excluded from further analysis due to a contamination of the culture. Terminal populations were spread on modified TA agar plates to isolate evolved clones based on differences in color and colony morphology. For each detected colony morphology (i.e., morphotype) that arose in one of the auxotrophic populations, four individual colonies were isolated as biological replicates for subsequent analyses. Isolates were stored at −80°C until further use.

Relative fitness of ancestral versus evolved populations

To determine whether and to which extent growth of evolved populations has changed in the course of the evolution experiment, fitness of derived genotypes relative to the one of the corresponding ancestor was determined. For this, cultures of evolved populations as well as their respective ancestors were inoculated from cryo-stocks and incubated separated from each other for 72 h in 4 mL MMAB medium. The number of colony-forming units (CFUs) was determined at 0 h and after 72 h by plating on modified TA agar.

Quantification of amino acid production levels using biosensors

To compare the amount of tyrosine or tryptophan that was produced by ancestral and evolved strains, both types were used as amino acid donor in coculture experiments with auxotrophic biosensor strains. Auxotrophic donors were supplemented with the required amino acid (150 μM), while WT cells were cultivated in unsupplemented minimal medium. Because the growth of biosensors depended on the amount of amino acid provided by the donor, biosensor growth can be used as an integrative measure to quantify the amount of amino acid produced by the donor genotype [43]. For this, the generated strains *E. coli* Δ*tyrA* Δ*araDAB lacZ camR* and *E. coli* Δ*trpB* Δ*araDAB lacZ camR* were used as biosensors, since their numbers could be determined in coculture with a donor - even at a low frequency. Cocultures of donors and amino acid biosensors were inoculated in a 1:1 ratio in 1 mL MMAB medium and incubated for 72 h. The number of CFUs of donor and biosensor was determined at 0 h as well 72 h post inoculation by plating. To phenotypically discriminate both types, populations were plated on either LB agar plates containing x-Gal as well as IPTG (resulting in white and blue colonies, respectively) or TA agar plates (resulting in white and red colonies, respectively). In addition, cocultures were spread on LB agar containing chloramphenicol to determine cell numbers of biosensors in a very low abundance.

Cost of adaptation

To determine whether adaption of derived auxotrophs to their coevolved partner was costly, 30 isolated clones were cultivated in amino acid-supplemented minimal medium (150 μM) and their growth compared to the growth of their corresponding evolutionary ancestor cultivated under the same conditions. In this experiment, a reduced growth of derived clones will indicate a cost of adaptation. Growth kinetics were determined by measuring the optical density at 600 nm every 30 min for a total of 72 h in a Tecan F200pro plate reader (Tecan Group Ltd., Switzerland). Strains were cultivated in a 384-well plate containing 50 μl of medium per well. During each cycle (i.e., 30 min), the microtiter plate was shaken trice for 3 min. The resulting growth data was used to calculate the maximum growth rate (μ_{MAX} using six time points) and the maximum density achieved (OD_{MAX} using eight time points) with the Magellan

software 7.1 (Tecan Group Ltd., Switzerland). For a better comparison, values of evolved genotypes were divided by averaged values of their corresponding ancestors.

Contact-dependent growth

To determine whether physical contact between cells is necessary to facilitate the exchange of amino acids and thus enhance growth, interacting genotypes were cultivated in a device that allows to grow two populations of cells either in the same compartment or separated by a filter membrane (0.2 mm, polyethersulfone, Pall GmbH, Germany), which prevents a physical contact between cells, but allows a transfer of free amino acids through the extracellular environment (i.e., Nurmikko cells [34]). In this experiment, pairs of ancestral auxotrophic genotypes and consortia of derived genotypes were analyzed. In cases were multiple morphotypes have been detected, all isolated clones were mixed in equal ratios according to the auxotrophy-causing mutations. Each combination was replicated four times. The initial OD_{600nm} was set to 0.001 with each auxotrophy representing 50% of the initial population. In cases were multiple isolates have been isolated from the same derived population of cocultured auxotrophs, their initial density was adjusted such that their combined density reached an OD_{600nm} of 0.001 as well. Each Nurmikko cell contained 4 mL MMAB minimal medium and was incubated under shaking conditions (i.e., 150 rpm, 30°C). Total numbers of CFUs were determined after 0 h and 72 h incubation on modified TA agar.

Cluster formation

In order to determine the propensity of the differentially treated populations to form multicellular clusters, cultures were analyzed by laser diffraction spectroscopy. This technique utilizes diffraction patterns of a laser beam that is passed through a solution to precisely quantify particle size distributions. To this end, ancestral or derived populations of the three experimental groups (i.e., prototrophic WT, auxotrophic monocultures, and auxotrophic cocultures) were directly inoculated from cryo-stocks into glass bottles containing MMAB medium. Monocultures of auxotrophs were additionally supplemented with 50 μM of the respective amino acid. The total culture volume was adjusted to the optical density reached during the exponential growth phase (i.e., WT: 20 ml, auxotrophic monocultures: 50 ml, coculture: 100 ml). Due to the increased variation observed in test experiments, each coculture population (n = 10) was replicated three times, while each population of control groups was only replicated once (n = 12 for WT and n = 24 for auxotrophic monocultures). Cluster formation was verified for ancestral (0 days) and evolved populations (80 days). Analysis of particle size distribution was performed utilizing a Beckman Coulter LS 13 320 laser diffractometer with universal liquid module using the Fraunhofer optical model. If necessary, precultures were diluted until a sufficient obscuration (~5%) was reached. Analysis was performed with precultures in exponential growth phase with pump speed set to 6% to minimize shear forces that degrade cell clusters over time. Each sample was measured three times for one minute. Averaged output files of these individual measurements were used for further analysis.

Scanning electron microscopy

Precultures of wild type, auxotrophic monocultures, and auxotrophic cocultures were inoculated in 96-well plates containing 1 ml of unsupplemented or amino acid-supplemented MMAB medium and incubated for 20 h. Afterward, cells were pelleted and the media supernatant removed. To start cultures, scintillation vials containing 4 mL of minimal medium were inoculated to a final density of 0.005 OD_{600nm}. Monocultures of auxotrophs were supplemented with amino acids, while auxotrophic cocultures and populations of WT were cultivated in unsupplemented medium.

Samples were allowed to settle on coverslips (Thermo Scientific, Nunc, Thermanox) for 15 min and then fixed for 1 h with 2.5% glutaraldehyde and dehydrated with ethanol in serially increased concentration, followed by critical point drying with a Leica EM CPD300 Auto (Leica, Germany). Samples were sputter-coated with gold (layer thickness: 5.5 nm) in a Leica EM ACE600 high vacuum coater (Leica, Germany) and analyzed at different magnifications with a JEOL JSM-IT200 InTouchScop scanning electron microscope (Joel, Germany) at 15 kV acceleration voltage and a working distance of 8.8 mm using an in-lense secondary electron detector.

Invasion-from-rare experiment

To determine whether or not physical contact among cells was essential for newly evolved cooperative genotypes to increase in frequency, an invasion-from-rare experiment was conducted. For this, the invasion success of cooperative phenotypes within a population of non-cooperative auxotrophs was quantified using Nurmikko cells. Tripartite populations (i.e., two ancestral auxotrophs plus one invader – an evolved cooperator) were either grown separated by a filter membrane (based on their auxotrophy) or under conditions that allowed mixing among genotypes (i.e., without filter membrane). To determine baseline invasion levels using this assay, also the invasion success of ancestral cells was quantified as described above. Cooperative phenotypes were selected based on their ability to support the growth of a cocultured auxotrophic biosensor strain. In this way, six isolates were chosen with at least one representative for each of the four genotypic combinations of auxotrophy and phenotypic marker genes, which have been used in the evolution experiment. Two ancestral auxotrophs were used to found a coculture in a 1:1 ratio and an initial OD_{600nm} of 0.005, to which an invader (i.e., evolved or ancestral auxotroph) was added with a 0.05% initial frequency. Each combination including a particular invader was replicated five times and conditions were identical to the Nurmikko cell experiment mentioned above. CFUs were determined by plating during the onset of the experiment and after 72 h of incubation. To discriminate ancestral invaders in established tripartite consortia, cultures were plated on MMAB agar plates containing one of the required amino acids.

Further discrimination of the respective auxotroph (i.e., competitor) and the invader sharing the same auxotrophy required the use of indicator dyes in the respective MMAB agar plates as described above for the biosensor experiment. To determine low frequencies of invaders, plating was additionally performed on LB agar plates containing 50 μg ml^{-1} kanamycin.

Population dynamic model

To disentangle the effect of amino acid overproduction and cluster formation on the evolution of mutualistic cooperation, a population dynamics model of individual cells and cells in clusters was developed and analyzed. In this model, wild type and mutant cells differed significantly in their replication rate to reflect the differential cost of amino acid production in each case. Moreover, amino acid production and reciprocity within clusters increased cell replication through a positive feedback loop. Consequently, the fitness of a cell depended on i) whether or not it was part of a cluster and ii) the composition of the cluster (i.e., ratio of cooperative to non-cooperative cells). Clusters could increase in size via the growth of the constituent cells as well as by a 'coming together' process, where free-living cells attach to previously existing clusters.

We investigated the effect of cluster formation and amino acid production within clusters on the evolution of cooperation. Scenarios where amino acid production and cluster formation are both low, are characterized by a population consisting mainly of individual, free-living cells, with a small population size. Under these conditions, a mutation causing a cooperative overproduction of metabolites will decrease the average fitness and thus frequently drive the whole population to extinction. Therefore, cooperation cannot evolve if cluster formation is below a certain threshold and only individual cells are present. If cluster formation is high, but reciprocity between cells within clusters is low, cooperation cannot evolve either, and the population consists mainly of non-cooperative clusters. Our results show that only when the rate of cluster formation and amino acid production levels of cells within clusters and are both high, cooperation can evolve (Figure 5). In our model, we do not keep track of clusters that only contain one partner, as their fitness is expected to be too low and their role in the dynamics is negligible.

The full model is given by the following set of differential equations:

$$\frac{dx}{dt} = a\,x - \kappa x^2 - \beta x\,z_0 - \beta x\,z_x + \gamma z_0 + \gamma z_x - \mu x$$

$$\frac{dy}{dt} = a\,y - \kappa y^2 - \beta y\,z_0 - \beta y\,z_y + \gamma z_0 + \gamma z_y - \mu y$$

$$\frac{dx_m}{dt} = a_m\,x_m - \kappa x_m^2 - \beta x_m z_y - \beta x_m\,z_1 + \gamma z_y + \gamma z_1 + \mu x$$

$$\frac{dy_m}{dt} = a_m\,y_m - \kappa y_m^2 - \beta y_m z_x - \beta y_m\,z_1 + \gamma z_x + \gamma z_1 + \mu y$$

$$\frac{dz_0}{dt} = z_0\,(r\chi_0 + \beta x + \beta y - \gamma - \mu - K\,z_0 - d) + \mu_R\,(z_x - z_y)$$

$$\frac{dz_x}{dt} = z_x\left(\varphi r\chi_x + \beta x + \beta y_m - \gamma - \mu + \mu\frac{z_0}{z_x} - K\,z_x - d\right) + \mu_R\,(z_1 - z_x)$$

$$\frac{dz_y}{dt} = z_y\left(\varphi r\chi_y + \beta x_m + \beta y - \gamma - \mu + \mu\frac{z_0}{z_y} - K\,z_y - d\right) + \mu_R\,(z_1 - z_y)$$

$$\frac{dz_1}{dt} = z_1\left(\varphi r\chi_1 + \beta x_m + \beta y_m - \gamma + \mu\frac{z_x}{z_1} + \mu\frac{z_y}{z_1} - K\,z_1 - d - 2\,\mu_R\right)$$

Individual '*wild type*' cells are given by variables x and y, representing the two different partners, while individual '*mutant*' cells are given by variables x_m and y_m for each partner, respectively. The replication rate of cells outside clusters is given by parameters α and α_m for wild types and mutants. Individual free-living cells are assumed to have a logistic growth, with a rate of self-limitation given by parameter κ. Events where individual cells join a cluster occur at a rate β, contributing to cluster formation. Cells mutate from non-cooperators into cooperators at a rate μ.

The number of cells in clusters is given by variable z_p. The subscript p refers to the type of cluster ($p = (0, x, y, 1)$). From this result four types of clusters including clusters that mainly contain non-cooperating cells (z_0), clusters that mainly consist of one cooperative auxotroph (z_x, z_y), and clusters, where both partners are cooperators (z_1). Reciprocal interactions between cells in clusters can increase cell replication above baseline levels (r) via a positive feedback loop. The enhanced replication rate resulting from this process is also affected by the baseline amino acid production rate (φ) as well as the specific amino acid production rate for each cluster type (χ_p). Cooperators in clusters can revert to non-cooperation at a rate μ_R. In our implementation of the model, we set the rate at which a mutation deactivates a cooperative phenotype (μ_R) to be two orders of magnitude above the rate at which a non-cooperator turns into a cooperating cell (μ). This rather conservative approach was used to challenge the proposed evolutionary mechanism by limiting the supply of cooperative mutants. Cells in clusters were assumed to have a logistic growth, with a rate of self-limitation given by parameter K. Mutations can occur within clusters, leading to a process, where clusters of one type can form clusters of a different type. Clusters release cells at a rate γ and cells within clusters die at a rate d. Given that our model describes the dynamics of cells in clusters and not cell clusters themselves, events that do not directly affect cell growth are not explicitly included in the model. For example, the number of clusters can increase by cluster fission, but this event will in itself not affect the number of cells in clusters. Therefore, our approach is consistent with processes occurring on a cluster-level (e.g., cluster fission and fusion) without explicitly accounting for them in the model.

We analyzed a deterministic as well as a stochastic dynamic of the model. The stochastic dynamic of the model was implemented using the Gillespie algorithm, which allowed us to study the evolution of the allele frequency of cooperators in scenarios, in which only single cells are present. In this case, although cooperation can emerge, the cooperation alleles frequently go extinct, because of the small population sizes.

QUANTIFICATION AND STATISTICAL ANALYSIS

Relative fitness

The Malthusian parameter M [69] was used to describe the reproductive capacity of a given number of individuals during a certain period of time. M was calculated as a measure for fitness of evolved populations (*Evo*) relative to their respective ancestor (*Anc*) as:

$$M_{\mathrm{Evo}}/M_{\mathrm{Anc}} = \ln(N_{\mathrm{f,Evo}} / N_{\mathrm{i,Evo}})/ln\ (N_{\mathrm{f,Anc}}, / N_{\mathrm{i,Anc}})$$

with N_i representing the initial number of CFUs and N_f the final CFU-count after 72 h. Each evolutionary lineage was analyzed using six replicates.

Amino acid production levels

The net growth of amino acid biosensors in the presence of an evolved (D_{Evo}) or ancestral (D_{Anc}) donor cell was determined by subtracting the initial count (0 h) from CFU numbers after 72 h. Afterward, the resulting values were normalized per donor cell, to control for the effect of donor growth on biosensor growth measurements. The final results of this experiment were expressed as relative biosensor growth (ΔB), for which the normalized net growth values of biosensors that have been cocultivated with a derived donor (B_{Evo}), were divided by the corresponding values obtained from cocultures with ancestral donor genotypes (B_{Anc}). Thus, relative biosensor growth levels were calculated as follows:

$$\Delta B = \left(\left(\mathrm{CFU\ B_{Evo(72\ h)}} - \mathrm{CFUB_{Evo(0\ h)}}\right) / \left(\mathrm{CFUD_{Evo(72\ h)}} - \mathrm{CFUD_{Evo(0\ h)}}\right)\right) / \left(\left(\mathrm{CFUB_{Anc(72\ h)}} - \mathrm{CFUB_{Anc(0\ h)}}\right) / \left(\mathrm{CFUD_{Anc(72\ h)}} - \mathrm{CFUD_{Anc(0\ h)}}\right)\right)$$

The experiment was replicated three times for each ancestral population as well as each isolated clone from evolved cocultures.

Invasion success

First, the invasion success was determined as:

$$\text{Invasion success} = \left(\left(\mathrm{CFUInvader_{(72\ h)}} / \mathrm{CFUInvader_{(0\ h)}}\right) / \left(\mathrm{CFUCompetitor_{(72\ h)}} / \mathrm{CFUCompetitor_{(0\ h)}}\right)\right)$$

Second, the number of generations was calculated:

$$\text{Number of generation} = \left(\ln(\mathrm{CFU}\ 72\ h) - \ln\left(\mathrm{CFU}\ 0\ \mathrm{h}\right) / \ln(2)\right)$$

Third, the invasion success per generation was estimated as the change in final invader-to-competitor ratio over three days divided by the number of generations populations achieved during this time.

Statistical analysis

Normal distribution of data was analyzed using Kolmogorov-Smirnov tests. Homogeneity of variances was determined by applying Levene's test and variances were considered to be homogeneous when $p > 0.05$. Non-parametric tests were used when data was not normally distributed or variances were inhomogeneous. Statistical test procedures used and sample size (n) are specified in the results section, figure captions, and STAR Methods. In all cases, n refers to the number of independently replicated bacterial

populations. Asterisks indicate significant differences in pairwise comparisons (* $p < 0.05$, ** $p < 0.01$, *** $p < 0.001$). In boxplots, the thick line indicates the median of values, the box the 25th and 75th percentiles, and the whiskers 1.5x the interquartile range from the 25th to the 75th percentile. Unless specified otherwise in the figure legend, data is displayed as mean values ± 95% confidence interval. No statistical methods were used to predetermine sample size and the experiments were not randomized. Statistical analyses were performed using SPSS (version 25) and R (https://cran.r-project.org/).